Mineralogical Magazine, April 2015, Vol. 79(2), pp. 413–423

Imayoshiite, $Ca_3Al(CO_3)[B(OH)_4](OH)_6{\cdot}12H_2O$, a new mineral of the ettringite group from Ise City, Mie Prefecture, Japan

D. Nishio-Hamane[1,*], M. Ohnishi[2], K. Momma[3], N. Shimobayashi[4], R. Miyawaki[3], T. Minakawa[5] and S. Inaba[6]

[1] Institute for Solid State Physics, the University of Tokyo, Kashiwa, Chiba 277-8581, Japan
[2] 12-43 Takehana Ougi-cho, Yamashina-ku, Kyoto 607-8082, Japan
[3] Department of Geology and Palaeontology, National Museum of Nature and Science, Tsukuba 305−0005, Japan
[4] Department of Geology and Mineralogy, Graduate School of Science, Kyoto University, Kitashirakawa Oiwake-cho, Sakyo-ku, Kyoto 606-8502, Japan
[5] Department of Earth Science, Faculty of Science, Ehime University, Matsuyama, Ehime 790-8577, Japan
[6] Inaba-Shinju Corporation, Minamiise, Mie 516-0109, Japan

[*Received 28 May 2014; Accepted 17 September 2014; Associate Editor: P. Leverett*]

ABSTRACT

Imayoshiite, $Ca_3Al(CO_3)[B(OH)_4](OH)_6{\cdot}12H_2O$, occurs in cavities in the altered gabbro xenolith in the sepentinized dunite exposed at Suisho-dani, Ise City, Mie Prefecture, Japan. Imayoshiite is colourless and transparent with a vitreous lustre and its aggregates are white with a silky lustre. Imayoshiite has a white streak. Its Mohs hardness is 2−3. It is brittle, the cleavage is distinct on {100} and the fracture is uneven. The mineral is uniaxial (−) with the indices of refraction $\omega = 1.497(2)$ and $\varepsilon = 1.470(2)$ in white light. Imayoshiite is hexagonal, $P6_3$, $a = 11.0264(11)$, $c = 10.6052(16)$ Å by powder diffraction and $a = 11.04592(2)$, $c = 10.61502(19)$ Å by single-crystal diffraction. The structural refinement converged to $R_1 = 2.35\%$. Imayoshiite is the first member of the ettringite group with both CO_3 and $B(OH)_4$ anions.

Keywords: imayoshiite, new mineral, ettringite group, crystal structure, Ise, Mie Prefecture.

Introduction

In 1985, during a mineralogical survey at the Ise-Shima region, Japan, one of the authors (S.I.) collected several white minerals with a silky lustre. Initial mineralogical investigations demonstrated that they were oyelite- and ettringite-group minerals (Minakawa *et al*., 1986). The latter has not yet been identified, although twelve ettringite-group minerals have been described to date. We have subsequently studied this unidentified mineral and revealed that it corresponds to a new species in the ettringite group.

The new mineral, imayoshiite, was named in honour of the Japanese mineral collector, Takaharu Imayoshi (1905−1984). His activities and specimens have undoubtedly made a significant contribution to mineralogy. He supported the geological and resource survey as a local guide, and helped with curation at the University of Tokyo after World War II. He also contributed to the promotion of geosciences by organizing an amateur mineralogy club in Tokyo, and one of the authors (S.I.) studied under his tutelage. His personal collection numbers ~10,000 specimens, and these are now stored and displayed in the Geological Museum, Geological Survey of Japan, AIST, where they are used for the study of mineralogy and its promotion. The mineral data and the name have

* E-mail: hamane@issp.u-tokyo.ac.jp
DOI: 10.1180/minmag.2015.079.2.18

FIG. 1. Photomicrograph of imayoshiite from Suisho-dani. It forms a fibrous aggregate with silky lustre.

been approved by the International Mineralogical Association Commission on New Minerals, Nomenclature and Classification (IMA 2013−069, Nishio-Hamane *et al*., 2013). The type specimen is deposited in the collections of the National Museum of Nature and Science, Japan, specimen number NSM−M43749 (holotype) and M43750 (cotype).

Occurrence

The Ise-shima region of the Shima Peninsula refers to the area of the eastern Mie Prefecture of Japan, and its geology consists of accretionary complexes within the Sambagawa, Chichibu and Shimanto Terranes. In the eastern Ise-shima region, the Mikabu belt, which is composed of mafic rocks, lies on the boundary between the Sambagawa and Chichibu Terranes. The Mikabu belt is exposed in the Suisho-dani valley, Ise City, Mie Prefecture, Japan (34º27′45N 136º43′55″E). In this area, the mafic rocks in the Mikabu belt consist mainly of sepentinized dunite and occasionally include xenoliths which consist of gabbro and its pegmatite. Rims of these xenoliths suffer hydrothermal alteration, and plagioclase, a main constituent of the xenoliths, has been altered to hydrous calcium silicate minerals such as oyelite, hydrogarnet, xonotlite, tobermorite, bultfonteinite, apophyllite and prehnite (Minakawa *et al*., 1986). Imayoshiite coexists with the above minerals in the cavities in this xenolith (Fig. 1) where it occurs as aggregates of fibrous-to-acicular crystals up to 2 mm across.

Physical and optical properties

Imayoshiite crystals are colourless and transparent with a vitreous lustre and its aggregates are white with a silky lustre. Imayoshiite has a white streak and its Mohs hardness is 2−3. It is brittle, the cleavage is distinct on {100} and the fracture is uneven. The mineral is uniaxial (−) with the indices of refraction $\omega = 1.497(2)$ and $\varepsilon = 1.470(2)$ in white light. No fluorescence was observed under longwave or shortwave ultraviolet radiation.

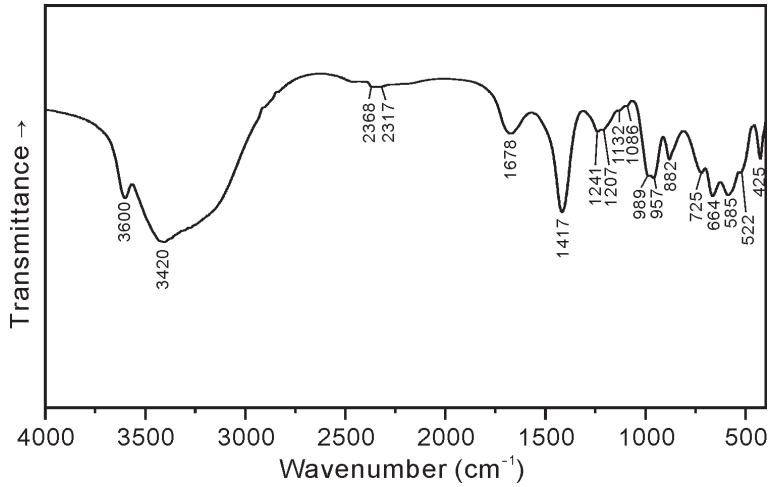

FIG. 2. IR spectrum of imayoshiite. The spectrum shows absorption bands at 3600 and 3420 cm^{-1} attributed to O−H stretching vibrations at 1678 cm^{-1} for the H−O−H bending vibrations, at 1417 and 882 cm^{-1} for the vibrations of the carbonate group and at 1207 cm^{-1} for the vibrations of $B(OH)_4$ tetrahedra.

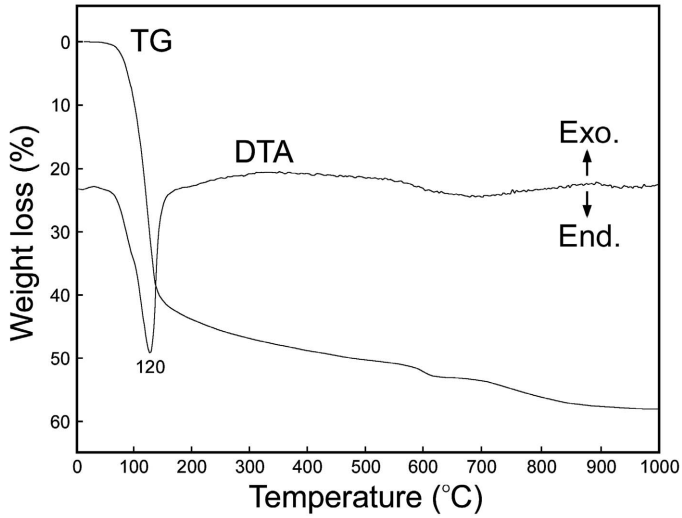

FIG. 3. TG and DTA curves for imayoshiite.

The density, 1.79 g cm^{-3}, was calculated on the basis of the empirical formula and unit-cell volume by powder X-ray diffraction (XRD).

Infrared spectra and thermal behaviour

A Fourier transform infrared (FTIR) absorption spectrum of imayoshiite was recorded with a KBr pellet method on a JASCO MFT−680 FTIR spectrometer for the region from 4000 cm^{-1} to 400 cm^{-1} (Fig. 2). The spectrum shows absorption bands at 3600 and 3420 cm^{-1} attributed to O−H stretching vibrations, at 1678 cm^{-1} to H−O−H bending vibrations, at 1417 and 882 cm^{-1} to the vibrations of the carbonate group and at 1207 cm^{-1} to the vibrations of $B(OH)_4$ tetrahedra.

Thermogravimetric (TG) and differential thermal analysis (DTA) curves are given in Fig. 3. The DTA curve has a strong endothermic peak at 120ºC corresponding to loss of water. The weight losses were 50.02% and 7.49% from room temperature to 500ºC and from 500ºC to 900ºC, respectively; these are attributed to the evolution of H_2O and CO_2, respectively.

Chemical composition

Table 1 shows the chemical composition of imayoshiite. Five chemical analyses were carried out using a JEOL JSM−5600 electron microprobe (energy dispersive spectroscopy mode, 15 kV,

TABLE 1. Chemical composition of imayoshiite.

	Wt.%	Range
CaO	28.20	27.17−29.13
Al_2O_3	7.60	7.35−8.03
SiO_2	1.17	1.11−1.29
SO_3	0.84	0.80−0.93
CO_2	7.49*	
B_2O_3	5.47†	
H_2O	50.02*	
Total	100.80	
Basis of 3 Ca		
Ca	3	
Al	0.889	
Si	0.116	
Total	4.005	
CO_3^{2-}	1.015	
$B(OH)_4^-$	0.937	
SO_4^{2-}	0.063	
Total	1	
$(OH)^-$	5.961	
O^{2-}	0.039	
H_2O	11.709	

* from TG data.
† calculated from stoichiometry.

0.4 nA, 5 μm beam diameter) for CaO, Al_2O_3, SiO_2 and SO_3. As IR spectroscopy confirmed the presence of B_2O_3, CO_2 and H_2O within the structure, B_2O_3 was estimated from the single-crystal XRD study as B + S = 1 atom per formula unit. CO_2 and H_2O were determined by TG analysis. The empirical formula, on the basis of 3 Ca, is $Ca_3Al_{0.889}Si_{0.116}(CO_3)_{1.015}[B(OH)_4]_{0.937}(SO_4)_{0.063}[(OH)_{5.961}O_{0.039}]_{\Sigma 6}\cdot 11.709H_2O$. The ideal formula is $Ca_3Al(CO_3)[B(OH)_4](OH)_6\cdot 12H_2O$, which requires Al_2O_3 8.44, CaO 27.84, CO_2 7.28, B_2O_3 5.76, H_2O 50.68, total 100 wt.%.

Crystallography

The powder XRD patterns for imayoshiite were collected using a synchrotron X-ray source on the NE1 beam line of PF-AR, KEK, Japan. This beam line provides a 30 μm diameter collimated beam of monochromatized X-ray radiation (λ = 0.413 Å). The XRD spectra were collected by the Debye-Scherrer method and recorded using an imaging plate detector. Powder XRD data are listed in Table 2. Unit-cell parameters refined from the powder data are a = 11.0264(11), c = 10.6052(16) Å and V = 1116.6(3) Å^3.

A single crystal of imayoshiite was mounted on a glass fibre, and the XRD measurement was made on a Rigaku R-AXIS RAPID curved imaging plate diffractometer using Mo$K\alpha$ radiation monochromated and focused by a VariMax confocal multilayer mirror. The Rigaku *RAPID AUTO* software package was used for processing the diffraction data, including the application of a

TABLE 2. Powder XRD data for imayoshiite.

h k l	I/I_0	$d_{obs.}$ (Å)	$d_{calc.}$ (Å)	*h k l*	I/I_0	$d_{obs.}$ (Å)	$d_{calc.}$ (Å)
1 0 0	100	9.5434	9.5491	2 0 4	5	2.3185	2.3179
1 0 1			7.0963	3 2 0, 2 3 0	2	2.1899	2.1907
1 1 0	18	5.5149	5.5132	2 2 3	30	2.1739	2.1738
0 0 2	1	5.3005	5.3026	3 2 1, 2 3 1	6	2.1451	2.1454
1 1 1	8	4.8918	4.8917	2 1 4, 1 2 4			2.1367
2 0 0	7	4.7778	4.7746	3 1 3, 1 3 3	23	2.1198	2.1196
1 0 2	40	4.6364	4.6358	4 1 0, 1 4 0	1	2.0839	2.0838
2 0 1	1	4.3528	4.3537	1 0 5	2	2.0710	2.0706
1 1 2	33	3.8217	3.8218	4 1 1, 1 4 1	3	2.0439	2.0447
2 1 0, 1 2 0			3.6092	3 0 4			2.0372
2 0 2	9	3.5484	3.5482	3 2 2, 2 3 2	9	2.0248	2.0247
2 1 1, 1 2 1	16	3.4171	3.4168	1 1 5	3	1.9794	1.9796
1 0 3	2	3.3156	3.3152	4 0 3			1.9784
3 0 0	4	3.1827	3.1830	4 1 2, 1 4 2	7	1.9395	1.9394
3 0 1	4	3.0497	3.0487	2 0 5			1.9384
2 1 2, 1 2 2	9	2.9773	2.9837	2 2 4	6	1.9100	1.9109
1 1 3			2.9759	5 0 0			1.9098
2 0 3	1	2.8410	2.8411	5 0 1	1	1.8794	1.8796
2 2 0	7	2.7558	2.7566	3 1 4, 1 3 4	1	1.8737	1.8737
3 0 2	31	2.7293	2.7291	3 2 3, 2 3 3	1	1.8623	1.8621
2 2 1	4	2.6675	2.6679	3 3 0			1.8377
0 0 4	11	2.6506	2.6513	2 1 5, 1 2 5	9	1.8288	1.8287
3 1 0, 1 3 0			2.6485	3 3 1	5	1.8106	1.8107
3 1 1, 1 3 1	12	2.5694	2.5695	4 2 0, 2 4 0			1.8046
1 0 4			2.5547	5 0 2	4	1.7964	1.7968
2 1 3, 1 2 3	69	2.5253	2.5255	4 1 3, 1 4 3			1.7951
2 2 2	1	2.4463	2.4458	4 2 1, 2 4 1	8	1.7781	1.7790
1 1 4	1	2.3834	2.3894	4 0 4			1.7741
4 0 0			2.3873	0 0 6	28	1.7677	1.7675
3 1 2, 1 3 2	4	2.3693	2.3694	1 0 6	8	1.7375	1.7380
3 0 3			2.3654	3 3 2			1.7364
4 0 1	1	2.3298	2.3290	5 1 0, 1 5 0	3	1.7153	1.7151

numerical absorption correction. The structure was solved by the charge flipping method using *Superflip* (Palatinus and Chapuis, 2007). Based on the symmetries of the electron density distribution calculated by *Superflip*, the non-centrosymmetric space group $P6_3$ was derived. For the refinement of the structure, *SHELXL-97* software (Sheldrick, 2008) was used with neutral-atom scattering factors. The unit-cell parameters are refined from 13,861 reflections exposed on 75 images with an oscillation angle of ω = 3º/frame: a = 11.04592(2), c = 10.61502(19) Å and V = 1121.65(4) Å^3. Details of the sample, data collection and structure refinement are provided in Table 3. The final atomic coordinates and equivalent isotropic atomic displacement parameters are summarized in Table 4. Anisotropic atomic displacement parameters, bond-valence analysis, selected interatomic distances and angles, and the hydrogen-bond geometry are listed in Tables 5, 6, 7 and 8, respectively.

The refined crystal structure of imayoshiite is shown in Fig. 4. The basic structure consists of columns and channels that are parallel to the c axis. The imayoshiite structure is based on $Ca_3[Al(OH)_6(H_2O)_{12}]$ columns consisting of $Al(OH)_6$ octahedra and the trimer of edge-sharing $Ca(OH)_4(H_2O)_4$ polyhedron. Carbon and B are independently located in channels that run parallel to the c axis, in the form of trigonal CO_3 and tetrahedral $B(OH)_4$, respectively. There is a slight orientational disorder of oxygens in the trigonal CO_3 into O71 and O72, which are related by 180º rotation around the c axis. There are also two possible orientations of $B(OH)_4$ tetrahedra related by inversion symmetry, and their distribution is totally disordered with 1/2 occupancies of the O8−O11 sites. A minor amount of sulfur also occupies the B site in the form of SO_4. When occupancy of B was freely refined, B + S was found to be close to 1. Positions of the hydrogen atoms were found by difference Fourier syntheses and

TABLE 3. Data-collection and structure-refinement details for imayoshiite.

Temperature	296(2) K
Radiation	Mo$K\alpha$ (λ = 0.71075 Å)
Crystal size (mm)	0.09 × 0.07 × 0.06
Space group	$P6_3$
Unit-cell dimensions	a = 11.0459(2), c = 10.61502(19) Å
	V = 1121.65(4) Å^3
Z	2
D_{calc}	1.790 g/cm^3
F000	636
Absorption coefficient (mm^{-1})	μ = 0.891
Diffractometer	R-AXIS RAPID
Voltage, Current	50 kV, 24 mA
2θ max (º)	60.0
No. of reflections measured	13,861
Independent reflections	2197 (R_{int} = 0.016, Friedel pairs: 1043)
Corrections	Lorentz-polarization, Absorption
Max. and min. transmission	0.9241−0.9485
Structure Solution	*Superflip* (Palatinus and Chapuis, 2007)
Refinement	Full-matrix least-squares on F^2
Function minimized	$\Sigma w(F_o^2 - F_c^2)^2$
Least-squares weights	$w = 1/ [\sigma^2(F_o^2) + (0.0369P)^2 + 0.2472P]$
	where $P = (\mathrm{Max}(F_o^2,0) + 2F_c^2)/3$
Anomalous dispersion	All non-hydrogen atoms
No. variables	113
Residuals: R_1 ($F^2 > 2\sigma(F^2)$)	0.0235
Residuals: R (All reflections)	0.0249
Residuals: wR_2 (All reflections)	0.0692
Goodness of fit indicator	1.259
Flack parameter (Friedel pairs = 1043)	0.00(5)
Largest diff. peak and hole	0.468 e/Å^3 and −0.282 e/Å^3

TABLE 4. Refined atomic position and isotropic displacement parameters (Å^2).

	x	*y*	*z*	U_{iso}*/U_{eq}	Occupancy
Ca1	0.00004 (3)	0.19606 (2)	0.24990 (14)	0.01439 (8)	1
Al1	0	0	0	0.01122 (12)	0.89Al +0.11Si
C1	⅓	⅔	0.4999 (4)	0.0167 (5)	1
B1	⅓	⅔	0.0005 (4)	0.0169 (5)	0.94B + 0.06S
O1	0.13511 (15)	0.13406 (15)	0.3900 (2)	0.0141 (3)	1
O2	0.13386 (14)	0.13484 (15)	0.1097 (2)	0.0140 (3)	1
O3	0.25892 (14)	0.41084 (13)	0.2578 (2)	0.0301 (3)	1
O4	0.00136 (16)	0.3443 (2)	0.4192 (3)	0.0351 (5)	1
O5	0.41082 (13)	0.25879 (14)	0.2418 (2)	0.0301 (3)	1
O6	0.3435 (2)	0.00100 (16)	0.0797 (3)	0.0339 (5)	1
O71	0.26642 (15)	0.53276 (13)	0.4995 (2)	0.0273 (3)	0.965 (3)
O72	0.206 (4)	0.611 (5)	0.484 (4)	0.027*	0.035 (3)
O8	0.1898 (3)	0.6190 (3)	0.0469 (3)	0.0236 (7)	0.515 (6)
O9	0.6189 (3)	0.1900 (3)	0.4533 (3)	0.0244 (8)	0.485 (6)
O10	⅓	⅔	0.8643 (5)	0.0298 (12)	0.515 (6)
O11	⅓	⅔	0.1350 (5)	0.0306 (12)	0.485 (6)
H1	0.2049	0.197	0.4312	0.053 (3)*	1
H2	0.1928	0.1974	0.0759	= U_{iso}(H1)	1
H31	0.2796	0.4564	0.335	= U_{iso}(H1)	1
H32	0.3063	0.3649	0.25	= U_{iso}(H1)	0.5
H41	0.0804	0.4146	0.4459	= U_{iso}(H1)	1
H42	−0.0721	0.3513	0.4434	= U_{iso}(H1)	1
H51	0.455	0.2793	0.1745	= U_{iso}(H1)	1
H52	0.3648	0.3108	0.25	= U_{iso}(H1)	0.5
H61	0.3513	−0.0721	0.0613	= U_{iso}(H1)	1
H62	0.4144	0.0721	0.0566	= U_{iso}(H1)	1

* refined with isotropic displacement parameter.

TABLE 5. Anisotropic displacement parameters (Å^2).

	U^{11}	U^{22}	U^{33}	U^{12}	U^{13}	U^{23}
Ca1	0.01831(12)	0.01440(12)	0.01175(12)	0.00914(9)	0.00052(15)	0.00018(18)
Al1	0.01276(16)	0.01276(16)	0.0081(2)	0.00638(8)	0	0
C1	0.0191(8)	0.0191(8)	0.0119(11)	0.0096(4)	0	0
B1	0.0139(7)	0.0139(7)	0.0228(12)	0.0070(4)	0	0
O1	0.0153(7)	0.0149(7)	0.0102(7)	0.0061(6)	−0.0001(6)	0.0002(6)
O2	0.0142(7)	0.0144(7)	0.0114(7)	0.0055(6)	−0.0009(6)	−0.0008(6)
O3	0.0356(6)	0.0252(5)	0.0286(7)	0.0145(5)	0.0033(8)	0.0011(7)
O4	0.0223(8)	0.0352(10)	0.0487(15)	0.0151(7)	−0.0035(6)	−0.0226(9)
O5	0.0256(5)	0.0359(6)	0.0280(7)	0.0149(5)	−0.0013(7)	−0.0032(8)
O6	0.0340(10)	0.0225(8)	0.0463(14)	0.0150(7)	0.0201(8)	0.0030(6)
O71	0.0246(6)	0.0178(6)	0.0368(6)	0.0085(5)	−0.0041(6)	0.0000(6)
O8	0.0174(11)	0.0231(13)	0.0291(15)	0.0092(10)	0.0042(10)	0.0010(11)
O9	0.0217(13)	0.0178(12)	0.0325(16)	0.0090(10)	−0.0020(11)	−0.0038(11)
O10	0.0342(17)	0.0342(17)	0.021(2)	0.0171(8)	0	0
O11	0.0344(18)	0.0344(18)	0.023(2)	0.0172(9)	0	0

TABLE 6. Bond-valence analysis for imayoshiite. The calculation is based on a crystal structure with ideal composition and atomic coordinates refined by single-crystal XRD using the bond-valence parameters (Brown and Altermatt, 1985). Hydrogen atoms were not considered in the calculation because their positions were not refined with adequate accuracy, and so the deviation of bond valemce sums (BVS) of oxygen sites from the ideal charges is due to the contribution of hydrogen bonds.

	— Ca —		Al	— C —		— B —		BVS	Charge
O1	0.283	0.295	0.480 (×3↓)					−1.06	−1
O2	0.293	0.282	0.488 (×3↓)					−1.06	−1
O3	0.157							−0.16	0
O4	0.289							−0.29	0
O5	0.157							−0.16	0
O6	0.287							−0.29	0
O71+O72				1.292 (O71)	0.053 (O72)			−1.35	−2
O8+O9						0.375 (O8)	0.365 (O9)	−0.74	−1
O10+O11						0.420 (O10)	0.415 (O11)	−0.84	−1
BVS	2.04		2.9	4.04		3.06			
Charge	2		3	4		3			

then fixed at the positions of the electron density peaks, because their coordinates could not be refined stably. Nevertheless, these hydrogen atoms form reasonable hydrogen-bond geometries and the H−O−H angles of water molecules are also acceptable (Table 8). Indeed, these hydrogen positions are basically consistent with those in the isostructural mineral (thaumasite) refined by single-crystal neutron diffraction (Gatta *et al*., 2012). The orientational disorder of the water molecules at O3 and O5 sites was also determined. Although two hydrogen sites exist around O3 and O5, they are too close to be occupied simultaneously. Therefore, the occupancies of H32 and H52 are limited to 1/2. Additional disordered hydrogen atoms bonded to O3, O5 and the $B(OH)_4$ molecule are also visible in

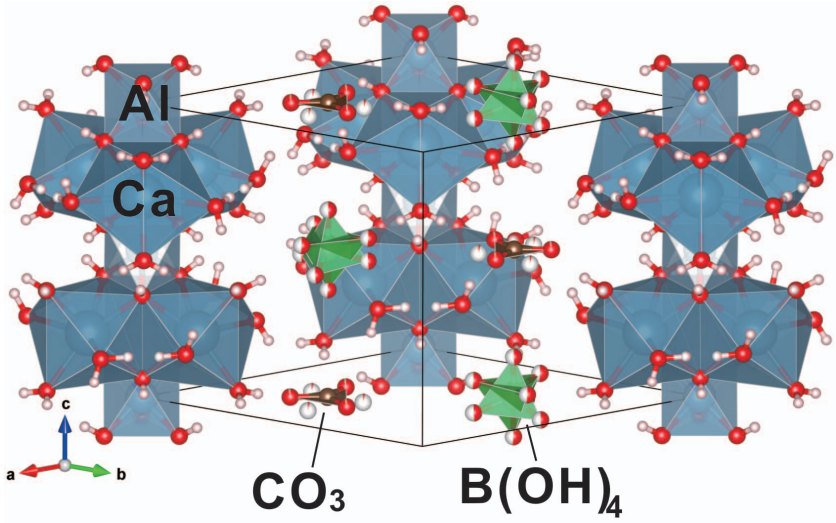

FIG. 4. Crystal structure of imayoshiite drawn using *VESTA* (Momma and Izumi, 2011). The imayoshiite structure is based on $Ca_3[Al(OH)_6(H_2O)_{12}]$ columns and CO_3 and $B(OH)_4$ in channels that run parallel to the *c* axis.

TABLE 7. Selected interatomic distances (Å) and angles (°) of imayoshiite.

Ca1–O1	2.4348(15)	Al1–O1^{iv}	1.8904(19)	C1–O71	1.2810(12)	B1–O8	1.483(3)
Ca1–O1^{i}	2.4197(15)	Al1–O1^{v}	1.8904(19)	C1–O71^{vii}	1.2810(12)	B1–O8^{vii}	1.483(3)
Ca1–O2	2.4201(15)	Al1–O1^{vi}	1.8904(19)	C1–O71^{viii}	1.2810(12)	B1–O8^{viii}	1.483(3)
Ca1–O2^{i}	2.4349(15)	Al1–O2	1.8863(19)	C1–O72	1.23(4)	B1–O9^{v}	1.483(3)
Ca1–O3	2.6512(13)	Al1–O2^{i}	1.8864(19)	C1–O72^{vii}	1.23(4)	B1–O9^{x}	1.483(3)
Ca1–O4	2.427(2)	Al1–O2^{iii}	1.8863(19)	C1–O72^{viii}	1.23(4)	B1–O9^{xi}	1.483(3)
Ca1–O5^{i}	2.6509(13)					B1–O10^{ix}	1.446(7)
Ca1–O6^{i}	2.429(2)					B1–O11	1.428(7)
O1–Ca1–O2^{i}	108.00(4)	O1^{iv}–Al1–O1^{vi}	85.85(9)	O71–C1–O71^{vii}	119.999(4)	O8–B1–O8^{vii}	109.5(2)
O1–Ca1–O3	72.17(5)	O1^{iv}–Al1–O1^{v}	85.85(9)	O71^{viii}–C1–O71	120.001(3)	O8–B1–O8^{viii}	109.5(2)
O1–Ca1–O5^{i}	136.42(6)	O1^{v}–Al1–O1^{vi}	85.85(9)	O71^{viii}–C1–O71^{vii}	119.997(4)	O8–B1–O9^{v}	144.15(13)
O1^{i}–Ca1–O1	64.07(7)	O2–Al1–O1^{iv}	179.41(7)	O72–C1–O71	64(2)	O8–B1–O9^{x}	103.75(13)
O1^{i}–Ca1–O2	108.47(4)	O2–Al1–O1^{v}	93.73(5)	O72–C1–O71^{vii}	56(2)	O8–B1–O9^{xi}	44.61(13)
O1^{i}–Ca1–O2^{i}	75.60(3)	O2–Al1–O1^{vi}	94.53(5)	O72–C1–O71^{viii}	171(2)	O8^{vii}–B1–O8^{viii}	109.5(2)
O1^{i}–Ca1–O3	133.10(6)	O2–Al1–O2^{i}	85.90(9)	O72^{vii}–C1–O71	171(2)	O8^{vii}–B1–O9^{v}	103.75(13)
O1^{i}–Ca1–O4	86.56(7)	O2^{i}–Al1–O1^{iv}	93.73(5)	O72^{vii}–C1–O71^{vii}	64(2)	O8^{vii}–B1–O9^{x}	44.61(13)
O1^{i}–Ca1–O5^{i}	74.49(5)	O2^{i}–Al1–O1^{v}	94.53(5)	O72^{vii}–C1–O72	118.2(10)	O8^{vii}–B1–O9^{xi}	144.15(13)
O1^{i}–Ca1–O6^{i}	147.72(5)	O2^{i}–Al1–O1^{vi}	179.41(7)	O72^{vii}–C1–O71^{viii}	56(2)	O8^{viii}–B1–O9^{v}	44.61(13)
O2–Ca1–O1	75.59(3)	O2^{iii}–Al1–O2	85.89(9)	O72^{vii}–C1–O72^{viii}	118.2(10)	O8^{viii}–B1–O9^{x}	144.15(13)
O2–Ca1–O2^{i}	63.94(7)	O2^{iii}–Al1–O2^{i}	85.90(9)	O72^{viii}–C1–O71	56(2)	O8^{viii}–B1–O9^{xi}	103.75(13)
O2–Ca1–O3	74.54(5)	O2^{iii}–Al1–O1^{iv}	94.53(5)	O72^{viii}–C1–O71^{vii}	171(2)	O9^{x}–B1–O9^{v}	109.2(2)
O2–Ca1–O4	147.74(5)	O2^{iii}–Al1–O1^{v}	179.41(6)	O72^{viii}–C1–O71^{viii}	64(2)	O9^{x}–B1–O9^{xi}	109.2(2)
O2–Ca1–O5^{i}	133.02(6)	O2^{iii}–Al1–O1^{vi}	93.73(5)	O72^{viii}–C1–O72	118.2(10)	O9^{xi}–B1–O9^{v}	109.2(2)
O2–Ca1–O6^{i}	86.31(7)					O10^{ix}–B1–O8	109.4(2)
O2^{i}–Ca1–O3	136.34(6)					O10^{ix}–B1–O8^{vii}	109.4(2)
O2^{i}–Ca1–O5^{i}	72.21(5)					O10^{ix}–B1–O8^{viii}	109.4(2)
O4–Ca1–O1	86.54(7)					O10^{ix}–B1–O9^{v}	70.3(2)
O4–Ca1–O2^{i}	148.26(5)					O10^{ix}–B1–O9^{x}	70.3(2)
O4–Ca1–O3	74.50(5)					O10^{ix}–B1–O9^{xi}	70.3(2)
O4–Ca1–O5^{i}	77.86(5)					O11–B1–O8	70.6(2)
O4–Ca1–O6^{i}	95.85(5)					O11–B1–O8^{vii}	70.6(2)
O5^{i}–Ca1–O3	138.33(4)					O11–B1–O8^{viii}	70.6(2)
O6^{i}–Ca1–O1	148.13(5)					O11–B1–O9^{v}	109.7(2)
O6^{i}–Ca1–O2^{i}	86.34(7)					O11–B1–O9^{x}	109.7(2)
O6^{i}–Ca1–O3	77.87(5)					O11–B1–O9^{xi}	109.7(2)
O6^{i}–Ca1–O5^{i}	74.59(5)					O11–B1–O10^{ix}	179.998(1)

Symmetry codes: (i) $-y, x-y, z$; (ii) $-x, -y, z+½$; (iii) $-x+y, -x, z$; (iv) $-x, -y, z-½$; (v) $x-y, x, z-½$; (vi) $y, -x+y, z-½$; (vii) $-x+y, -x+1, z$; (viii) $-y+1, x-y+1, z$; (ix) $x, y, z-1$; (x) $-x+1, -y+1, z-½$; (xi) $y, -x+y+1, z-½$; (xii) $x-y+1, x, z+½$; (xiii) $-x+1, -y+1, z+½$; (xiv) $x, y, z+1$; (xv) $y, -x+y+1, z+½$; (xvi) $x-y, x, z+½$.

TABLE 8. Hydrogen-bond geometry of imayoshiite.

D–H···*A*	D–H (Å)	H···*A* (Å)	*D*···*A* (Å)	*D*–H···*A* (º)
O1–H1···O6	0.8562(17)	2.226(3)	3.059(3)	164.26(16)
O2–H2···O4	0.7617(17)	2.337(3)	3.071(3)	162.29(19)
O3–H31···O71	0.928(2)	1.976(2)	2.879(3)	163.88(10)
O3–H32···O5	0.8966(13)	2.0168(13)	2.9126(17)	177.0(2)
O4–H41···O71	0.8760(17)	1.8888(15)	2.745(2)	165.38(13)
O4–H41···O72	0.8760(17)	1.95(5)	2.76(4)	153.5(14)
O4–H42···O8	0.8904(17)	1.852(3)	2.704(3)	159.5(2)
O4–H42···O9	0.8904(17)	1.886(3)	2.729(3)	157.2(2)
O5–H51···O71	0.831(2)	2.081(2)	2.885(3)	162.89(11)
O5–H52···O3	0.9424(13)	1.9718(13)	2.9126(17)	175.89(15)
O6–H61···O8	0.8758(17)	1.890(3)	2.730(3)	160.14(18)
O6–H61···O9	0.8758(17)	1.883(3)	2.702(3)	154.8(2)
O6–H62···O71	0.8217(18)	1.9684(15)	2.749(2)	158.42(14)

the difference Fourier, but cannot be assigned definitively at the present resolution due to their low occupancies. Although total hydrogen atoms in the refined structural model are slightly less than the number in the ideal composition, the *R* factor for the structural refinement was successfully converged: R_1 = 2.35%.

Relationship to other minerals

The formula of the ettringite-group mineral can be described basically as $Ca_3M(OH)_6R_{1.5-4}{\cdot}nH_2O$ (basis of 3 Ca), where *M* cations are Al^{3+}, Cr^{3+}, Fe^{3+}, Si^{4+}, Mn^{4+} or Ge^{4+} and *R* anions are SO_4^{2-}, CO_3^{2-}, SO_3^{2-}, PO_3OH^{2-} or $B(OH)_4^-$ (Table 9).

TABLE 9. Comparative data for ettringite-group minerals.

Mineral	Simplified formula*	*a* (Å)	*c* (Å)	Space group	Reference
Imayoshiite	$Ca_3Al(CO_3)[B(OH)_4](OH)_6{\cdot}12H_2O$	11.03	10.61	$P6_3$	This study
Thaumasite	$Ca_3Si(OH)_6(SO_4)(CO_3){\cdot}12H_2O$	11.05	10.41	$P6_3$	1
Jouravskite	$Ca_3Mn^{4+}(SO_4)(CO_3)(OH)_6{\cdot}12H_2O$	11.06	10.50	$P6_3$	2
Hielscherite	$Ca_3Si(SO_4)(SO_3)(OH)_6{\cdot}11H_2O$	11.11	10.49	$P6_3$	3
Micheelsenite	$(Ca,Y)_3Al(PO_3OH)CO_3(OH)_6{\cdot}12H_2O$	10.83	10.52	$P6_3$	4
Ettringite	$Ca_3Al(SO_4)_{1.5}(OH)_6{\cdot}13H_2O$	11.23	21.48	$P31c$	5
Sturmanite	$Ca_3Fe^{3+}(SO_4)_{1.5}[B(OH)_4]_{0.5}(OH)_6{\cdot}12H_2O$	11.19	21.91	$P31c$	6
Buryatite	$Ca_3(Si,Fe^{3+},Al)SO_4B(OH)_4(OH,O)_6{\cdot}12H_2O$	11.14	20.99	$P31c$	7
Charlesite	$Ca_3(Al,Si)(SO_4)[B(OH)_4]_{0.5}(OH,O)_6{\cdot}13H_2O$	11.16	21.21	$P31c$	8
UM**	$Ca_3Al(CO_3,SO_4)[B(OH)_4]_{0.5}(OH,O)_6{\cdot}13H_2O$	11.10	21.22	$P31c$?	9
Carraraite	$Ca_3Ge(SO_4)(CO_3)(OH)_6{\cdot}12H_2O$	11.06	10.63	$P6_3/m$	10
Kottenheimite	$Ca_3Si(SO_4)_2(OH)_6{\cdot}12H_2O$	11.15	10.57	$P6_3/m$	11
Bentorite	$Ca_3Cr(SO_4)_{1.5}(OH)_6{\cdot}13H_2O$	22.35	21.41	$P6_3/mmc$	12

* Basis of 3 Ca.
** Unamed mineral.
References: 1, Gatta *et al*. (2012); 2, Granger and Protas (1969); 3, Pekov *et al*. (2012); 4, McDonald *et al*. (2001); 5, Goetz-Neunhoeffer and Neubauer (2006); 7, Malinko *et al*. (2001); 8, Dunn *et al*. (1983); 9, Kusachi *et al*. (2008); 10, Merlino and Orlandi (2001); 11, Chukanov *et al*. (2012); 12, Gross (1980).

The structure consists of the $Ca_3[M(OH)_6(H_2O)_{12}]$ columns and *R* anions in channels, and the structure types are divided into four space groups. The component and the arrangement of *R* anions in $P6_3$ and $P31c$ structures are compared in Fig. 5 using several ettringite group examples. There are two distinct *R* anion sites and each site can be orientationally disordered in the $P6_3$ symmetry (Fig. 5). Imayoshiite corresponds compositionally to the Al- and $B(OH)_4$-dominant analogues of thaumasite and jouravskite of $P6_3$. Although the orientational disorder of the tetrahedron as $B(OH)_4$ is found in imayoshiite, the tetrahedron as SO_4 is ordered in the latter mineral. In $P31c$ symmetry such as shown by ettringite and sturmanite, there are four distinct anion sites and each site also allows the disorder and a H_2O molecule (Fig. 5). Kusachi *et al*. (2008) reported the unnamed mineral as the CO_3-rich charlesite which has the ettringite-type unit cell, $Ca_3Al(CO_3,SO_4)[B(OH)_4]_{0.5}(OH,O)_6{\cdot}13H_2O$ (basis of 3 Ca). This unnamed mineral is compositionally similar to imayoshiite, but these two are distinguishable using detailed composition and structure. Imayoshiite has an equal amount of CO_3 and $B(OH)_4$, while the unnamed mineral has the composition of CO_3:$B(OH)_4$ = 2:1 and the *c* axis doubled with respect to that of imayoshiite. Although structural analysis of charlesite and the unnamed mineral has not been reported, their respective stoichiometry and unit-cell data suggest that *R* anions may be localized to four sites in association with water molecules, as displayed in ettringite. Regardless, imayoshiite is the first distinct member essentially having both CO_3 and $B(OH)_4$ anions in the ettringite group.

Acknowledgements

The authors thank T. Nagai for help with the synchrotron X-ray experiment (no. 2012G050).

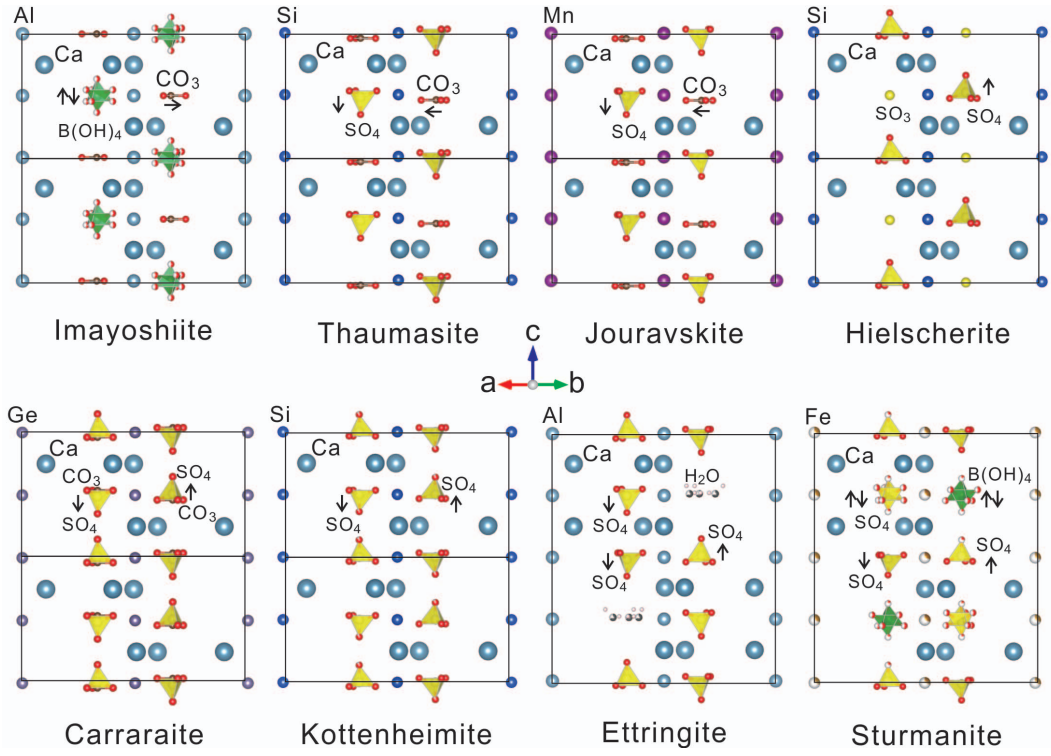

FIG. 5. A comparison of the component and arrangement of *R* anions in $P6_3$ and $P31c$ structures using several ettringite-group examples. The structures for imayoshiite, thaumasite, ettringite and sturmanite are are based on the present study, Gatta *et al*. (2012), Goents-Neunhoeffer and Neubauer (2006) and Pushcharovsky *et al*. (2004), respectively.

They are grateful to the anonymous referees for their constructive reviews.

References

Brown, I.D. and Altermatt, D. (1985) Bond-valence parameters obtained from a systematic analysis of the inorganic crystal-structure database. *Acta Crystallographica*, **B41**, 244–247.

Chukanov, N.V., Britvin, S.N., Van, K.V., Möckel, S. and Zadov, A.E. (2012) Kottenheimite, $Ca_3Si(OH)_6(SO_4)_2{\cdot}12H_2O$, a new member of the ettringite group from the Eifel area, Germany. *The Canadian Mineralogist*, **50**, 55–63.

Dunn, P.J., Peacor, D.R., Leavens, P.B. and Baum, J.L. (1983) Charlesite, a new mineral of the ettringite group, from Franklin, New Jersey. *American Mineralogist*, **68**, 1033–1037.

Gatta, G.D., McIntyre, G.J., Swanson, J.G. and Jacobsen S.D. (2012) Minerals in cement chemistry: a single-crystal neutron diffraction and Raman spectroscopic study of thaumasite, $Ca_3Si(OH)_6(CO_3)(SO_4){\cdot}12H_2O$. *American Mineralogist*, **97**, 1060–1069.

Goetz-Neunhoeffer, F. and Neubauer, J. (2006) Refined ettringite ($Ca_6Al_2(SO_4)_3(OH)_{12}{\cdot}26H_2O$) structure for quantitative X-ray diffraction analysis. *Powder Diffraction*, **21**, 4–11.

Granger, M.M. and Protas, J. (1969) Détermination et etude de la structure cristalline de la jouravskite $Ca_3Mn^{IV}(SO_4)(CO_3)(OH){\cdot}12(H_2O)$. *Acta Crystallographica*, **B25**, 1943–1951.

Gross, S. (1980) Bentorite. A new mineral from the Hatrurim area, west of the Dead Sea, Israel. *Israel Journal of Earth Science*, **29**, 81–84.

Kusachi, I., Shiraishi, N., Shimada, K., Ohnishi, M. and Kobayashi, S. (2008) CO_3-rich charlesite from the Fuka mine, Okayama Prefecture, Japan. *Journal of Mineralogical and Petrological Sciences*, **103**, 47–51.

Malinko, S.V., Chukanov, N.V., Dubinchuk, V.T., Zadov, A.E. and Koporulina, E.V. (2001) Buryatite $Ca_3(Si,Fe^{3+},Al)[SO_4][B(OH)_4](OH)_5O{\cdot}12H_2O$, a new mineral. *Zapiski Vserossijskogo Mineralogicheskogo Obshchestva*, **130**, 72–78.

McDonald, A.M., Peterson, O.V., Gault, R.A., Johnsen, O., Niedermayr, G., Brandstätter, F. and Giester, G. (2001) Micheelsenite, $(Ca,Y)_3Al(PO_3OH,CO_3)(CO_3)(OH)_6{\cdot}12H_2O$, a new mineral from Mont Saint-Hilaire, Quebec, Canada and the Nanna pegmatite, Narsaarsuup Qaava, South Greenland. *Neues Jahrbuch für Mineralogie, Monatshefte*, **2001**, 337–351.

Merlino, S. and Orlandi, P. (2001) Carraraite and zaccagnaite, two new minerals from the Carrara marble quarries: their chemical compositions, physical properties, and structural features. *American Mineralogist*, **86**, 1293–1301.

Minakawa, T., Inaba, S. and Noto, S. (1986) Oyelite from Suisho-dani, Ise, Mie Prefecture. *Journal of the Japanese Association of Mineralogist, Petrologists and Economic Geologists*, **81**, 138–142.

Momma, K. and Izuni, F. (2011) VESTA 3 for three-dimensional visualization of crystal, volumetric and morphology data. *Journal of Applied Crystallography*, **44**, 1272–1276.

Nishio-Hamane, D., Ohnishi, M., Momma, K., Shimobayashi, N., Miyawaki, R., Minakawa, T. and Inaba, S. (2013) Imayoshiite, IMA 2013-069. CNMNC Newsletter No. 18, December 2013, page 3251; *Mineralogical Magazine*, **77**, 3249–3258.

Palatinus, L. and Chapuis, G. (2007) SUPERFLIP – a computer program for the solution of crystal structures by charge flipping in arbitrary dimensions. *Journal of Applied Crystallography*, **40**, 456–462.

Pekov, I.V., Chukanov, N.V., Britvin, S.N., Kabalov, Y.K., Göttlicher, J., Yapaskurt, V.O., Zadov, A.E., Krivovichev, S.V., Schüller, W. and Ternes, B. (2012) The sulfite anion in ettringite-group minerals: a new mineral species hielscherite, $Ca_3Si(OH)_6(SO_4)(SO_3){\cdot}11H_2O$, and the thaumasite–hielscherite solid-solution series. *Mineralogical Magazine*, **76**, 1133–1152.

Pushcharovsky, D.Y., Lebedeva, Y.S., Zubkova, N.V., Pasero, M., Bellezza, M., Merlino, S. and Chukanov, N.V. (2004) The crystal structure of sturmanite. *The Canadian Mineralogist*, **42**, 723–729.

Sheldrick, G.M. (2008) A short history of SHELX. *Acta Crystallographica*, **A64**, 112–122.